Title

Characterization of the Relationship Between Intracranial Pressure and Electroencephalographic Monitoring in Burst-Suppressed Patients

Journal

Neurocritical Care, 22(2)

ISSN

1541-6933

Authors

Connolly, M
Vespa, P
Pouratian, N
et al.

Publication Date

2015-04-01

DOI

10.1007/s12028-014-0059-8

Peer reviewed

neurocritical care society Neurocrit Care (2015) 22:212–220
DOI 10.1007/s12028-014-0059-8

ORIGINAL ARTICLE

Characterization of the Relationship Between Intracranial Pressure and Electroencephalographic Monitoring in Burst-Suppressed Patients

Mark Connolly · Paul Vespa · Nader Pouratian · Nestor R. Gonzalez · Xiao Hu

Published online: 21 August 2014

Abstract
Background The objective of this study is to characterize the relationship between ICP and EEG
Methods Simultaneous ICP and EEG data were obtained from burst-suppressed patients and segmented by EEG bursts. Segments were categorized as increasing/decreasing and peak/valley to investigate relationship between ICP changes and EEG burst duration. A generalized ICP response was obtained by averaging all segments time-aligned at burst onsets. A vasodilatation index (VDI) was derived from the ICP pulse waveform and calculated on a sliding interval to investigate cerebrovascular changes post-burst.
Results Data from two patients contained 309 bursts. 246 ICP segments initially increased, of which 154 peaked. 63 ICP segments decreased, and zero reached a valley. The change in ICP (0.54 ± 0.85 mmHg) was significantly correlated with the burst duration ($p < 0.001$). Characterization of the ICP segments showed a peak at 8.1 s and a return to baseline at 14.7 s. The VDI for increasing segments was significantly elevated (median 0.56, IQR 0.31, $p < 0.001$) and correlated with burst duration ($p < 0.001$).
Conclusions Changes in the ICP and pulse waveform shape after EEG burst suggest that these signals can be related within the context of neurovascular coupling.
Significance Existence of a physiological relationship between ICP and EEG may allow the study of neurovascular coupling in acute brain injury patients.

Keywords Neurovascular coupling · Intracranial pressure · Electroencephalogram · Multi-modality monitoring · Acute brain injury

M. Connolly · P. Vespa · N. Pouratian · N. R. Gonzalez · X. Hu
Department of Neurosurgery, David Geffen School of Medicine, University of California, Los Angeles, CA, USA

X. Hu (✉)
Departments of Physiological Nursing/Neurosurgery, Institute for Computational Health Sciences, University of California San Francisco, San Francisco, CA 94143-0610, USA
e-mail: XHu@mednet.ucla.edu

X. Hu
Institue of Computational Health Sciences, University of California San Francisco, San Francisco, CA, USA

Introduction

After suffering a traumatic, ischemic, or hemorrhagic insult, the brain is susceptible to a multitude of secondary complications that can cause further injury. One such complication is elevated intracranial pressure (ICP) which can cause neurologic damage through ischemia and herniation [5, 20]. Because of the life-threatening nature of this complication, ICP has become a routinely measured signal in critical patients [23]. Other sources of secondary injury such as seizures [9, 26, 27] and spreading depression [10] can be detected through the use of electroencephalography (EEG). As this modality is inexpensive and non-invasive, EEG monitoring can be readily utilized in many patients admitted to a neurointensive care unit.

Ideally, these two modalities would be integrated to provide additional information about the condition of the patients. However, there is no established physiological relationship upon which to conduct an integrated analysis of ICP and EEG. As ICP is directly related to the blood volume within the cranial vault, neurovascular coupling, the mechanism whereby local brain activity causes a subsequent increase in blood flow to the active region may

provide the link between these two signals. This is of critical importance, as injury to the brain can induce pathological neurovascular coupling with deleterious effects [3, 6, 7]. However, there is no established technique for the study of neurovascular coupling in the acute phase following a traumatic injury.

To establish a relationship between EEG and ICP as a measure of neurovascular coupling, we hypothesized that bursts of electrical activity detected by EEG would be followed by a transient increase in ICP, and that with the prolonged absence of EEG burst activity, the ICP would decrease. Moreover, we hypothesized that this early increase and eventual decrease in ICP are mediated by vasodilation and vasoconstriction, which has been shown to be detectable in the ICP pulse waveform changes [1, 12]. In this study, we characterize the immediate changes in ICP after an EEG burst, and the general pattern between EEG burst in terms of the ICP amplitude and pulse waveform changes.

Materials and Methods

Patients and Data

Time-synchronized continuous ICP and depth EEG waveforms were obtained from patients admitted to the neurocritical care unit at the UCLA Ronald Reagan Hospital. The depth EEG was a six-electrode strip placed adjacent to the extraventricular drain catheter. Depth EEG signals were recorded at 2000 Hz, and the ICP signals were recorded at 240 Hz and upsampled to match the sampling rate of the EEG recordings. All monitoring was performed as part of the care prescribed by the attending physicians. Use of their data was permitted under the protocol as approved by the UCLA Institutional Review Board.

For this initial characterization of the ICP response of neurovascular coupling, signals were manually selected that showed high levels of burst suppression (burst suppression ratio >0.7) to minimize the interaction between individual bursts.

Burst Segmentation

Depth EEG signals were low-pass filtered at 1 Hz and then the envelope of the filtered depth EEG was calculated and integrated over a 1.2-second running window using a Hilbert transform. Local peaks of the resultant time series were then identified to determine a threshold that is 20 % of the difference between the amplitudes of the largest peak and the smallest peak. Then an estimate of the burst onset and offset is identified as the first and the last point of an episode where the integrated envelope time series crosses the threshold and possesses a minimum gap of 300 ms to adjacent episodes. The onset was further fine-tuned to be the first point reaching the 97th percentile of the depth EEG amplitude of the episode starting at the offset of last burst and ending at the preliminary onset of the current burst. There is no need to adjust preliminary offsets (Fig. 1).

Characterization of the ICP Changes During Burst and Suppression

The ICP waveform was low-pass filtered at 0.2 Hz to remove the frequencies associated with the cardiac pulsation and the intra-pulse oscillations. To remove the respiratory component of the ICP waveform, the peak in frequency spectrum of the waveform between 0.15 and 0.4 Hz was programmatically identified and the appropriate frequencies band-stop filtered.

To categorize the ICP segments, it was first determined whether a peak or valley existed in the suppression interval by identifying a point that was either higher or lower than both endpoints. Segments with a peak were categorized as increasing and those with a valley were classified as decreasing. For ICP segments that did not contain a peak or valley, the two endpoints were compared to determine whether the segment was increasing or decreasing.

To test the hypothesis that electrical activity (EEG burst) is associated with a transient increase in ICP, the following features were quantified:

- The occurrence of ICP segments with initial increases versus ICP with initial decreases
- The magnitude of the ICP increase after a burst
- The correlation between burst duration and the ICP increase

To characterize the ICP amplitude changes during the suppression interval, the ICP segments were aligned by the onset of the preceding EEG burst, calibrated by shifting up or down such that the mean value of each individual segment was 0.0 mmHg. The mean value and 95 % confidence interval of the combined ICP responses were then calculated to produce a generalized ICP response.

Characterization of Vasodilation During Burst and Suppression

To investigate whether the transient changes in ICP were caused by vasodilation we utilized our recently developed morphological clustering and analysis of ICP (MOCIAP) and pulse morphological template matching (PMTM) algorithms [1, 2, 12]. MOCAIP computes 128 ICP pulse waveform metrics from an ICP pulse, and PMTM computes the metric trends and compares them to a template obtained from patients given CO_2 to produce hypercapnic

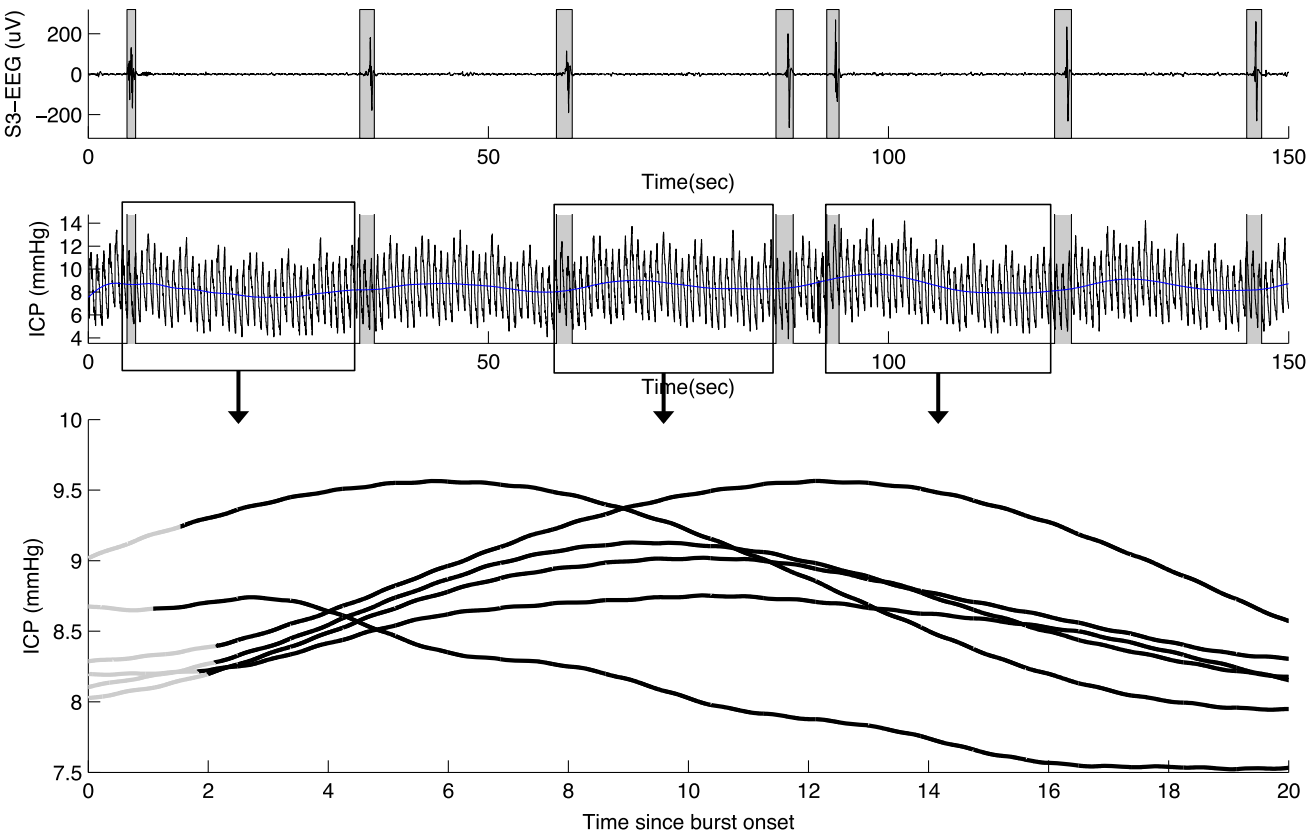

Fig. 1 The segmentation of ICP based on EEG burst activity. *Top* A sample EEG segment with the identified periods of EEG bursts activity highlighted in *grey*. *Middle* Raw ICP in *black* with filtered ICP overlaid. Box outlines show example ICP between each burst onset. *Bottom* Segments of filtered ICP during EEG burst (*grey*) and after (*black*)

vasodilation. In this template, 50 metrics have increasing trends, 22 have decreasing trends, and the rest have no significant trend. With this information, PMTM can determine to what extent the changes in the ICP waveform correspond to those of patients undergoing hypercapnic vasodilation. The vasodilation index (VDI) is expressed as the proportion of metric trends that agree between the experimental data and template.

The VDI was calculated for each ICP increase following an EEG burst. To test the hypothesis that the coupling between EEG activity and ICP increases is mediated by vasodilation the following relationships were quantified:

- The VDI during ICP increases, compared to the VDI for randomly selected ICP segments with similar lengths
- The correlation between the VDI in the interval immediately after the EEG burst and the duration of the burst

To characterize the vasoreactivity changes during the suppression interval, the VDI was calculated on a 2-s sliding window with a 1 s shift between the onsets of each EEG burst. Each window was compared with a distribution of VDI values calculated from randomly selected ICP segments of a similar length.

Statistics and Analysis

VDI values, which have non-normal distribution, were compared using Mann–Whitney test. VDI comparisons were also made using a *t* test, which is presented below for clarity. Reported correlations are Spearman with corresponding significance tests. Statistical analyses were performed for each patient individually, and for all patients combined. All calculations were performed using MATLAB.

Results

Patients and Data

Data were collected for two female patients, age 38 and 53, undergoing ICP and depth EEG monitoring as part of their treatment of a traumatic brain injury (TBI) and an aneurysmal subarachnoid hemorrhage (aSAH), respectively.

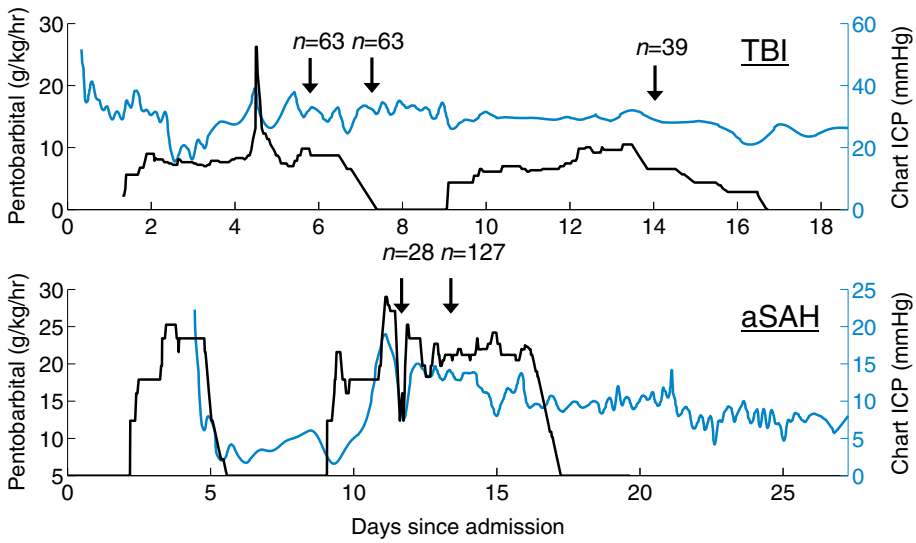

Fig. 2 Clinical course of the two patients including the ICP as recorded by nursing staff and the dose of pentobarbital

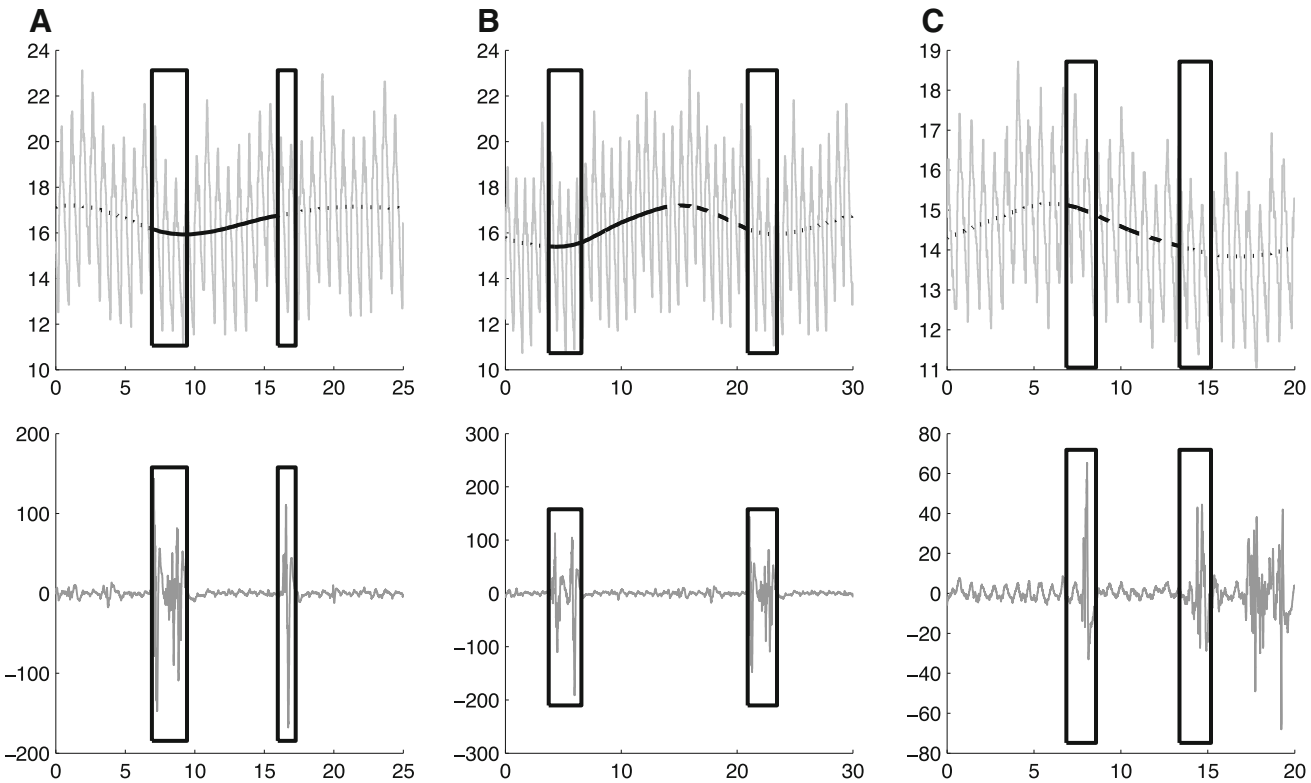

Fig. 3 The three ICP patterns observed after an EEG burst. **a** Increasing without a peak, observed after 92 bursts, **b** increasing with a peak, observed after 154 bursts and **c** decreasing without a valley, observed ofter 63 bursts

Both patients were burst suppressed with pentobarbital for treatment of refractory intracranial hypertension, which was unsuccessfully titrated once. The dataset includes ICP and depth EEG monitoring from 3 separate days for the TBI patient and 2 separate days for the aSAH patient. Total data length was 64 min (TBI 27 min, aSAH 37 min) and included 309 bursts (TBI 162 bursts, aSAH 147 bursts) (Fig. 2). Samples were collected during periods of maximal burst suppression.

ICP Categorization

Of the 309 bursts, 246 (79.6 %) were followed by an increase in ICP (TBI 131–80.9 %, aSAH 115–78.2 %). Of

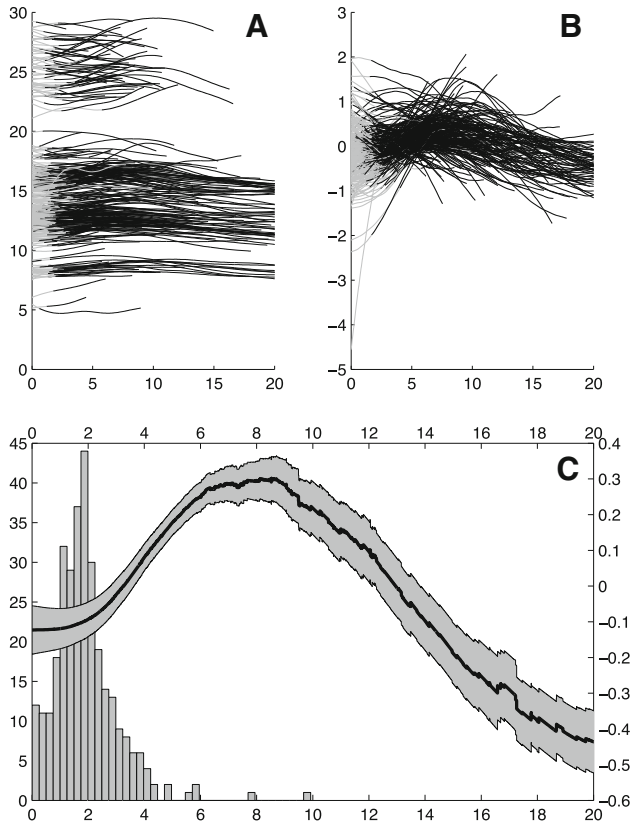

Fig. 4 The creation of the generalized ICP response to an EEG burst. **a** All ICP segments with corresponding burst duration in *grey*. **b** All ICP segments shifted such that the mean value is equal to zero. **c** The mean value of all aligned and calibrated ICP segments with 95 % confidence interval. Histogram shows the burst duration

the 246 increasing segments, 154 (62.9 %) had a peak in the ICP that was followed by a decrease in ICP (TBI 90–68.7 %, aSAH 64–55.7 %). A total of 63 (20.4 %) bursts were followed by a decrease in ICP (TBI 31–49.2 %, aSAH 32–50.8 %). No decreasing ICP segment changed direction before the onset of the next burst (Fig. 3).

ICP Amplitude Changes After EEG Burst

The mean change in ICP amplitude between the burst onset and the peak or onset of the next burst was 0.54 mmHg (TBI 0.58 mmHg and aSAH 0.50 mmHg) with a standard deviation of 0.85 mmHg (TBI 0.77 mmHg, aSAH 0.93 mmHg). For increasing ICP segments, the mean increase in ICP was 0.79 mmHg (TBI 0.81 mmHg, aSAH 0.77 mmHg). For decreasing segments, the mean decrease was 0.43 mmHg (TBI 0.41 mmHg and aSAH 0.46 mmHg).

Using a spearman correlation, the ICP amplitude change between the burst onset and the peak or onset of the next burst was significantly correlated with the duration of the EEG burst (All $\rho = 0.48$ $p < 0.001$, TBI $\rho = 0.49$ $p < 0.001$, aSAH $\rho = 0.48$ $p < 0.001$). For increasing ICP segments, the correlation was similar and also significant (All $\rho = 0.49$ $p < 0.001$, TBI $\rho = 0.53$ $p < 0.001$, aSAH $\rho = 0.47$ $p < 0.001$).

Time alignment (Fig. 4a) and calibration (Fig. 4b) of the ICP during the suppression interval allowed the characterization of the ICP response curve (Fig. 4c). The mean curve has a change in ICP amplitude of 0.45 mmHg between burst onset and the peak. The peak is reached 8.1 s after burst onset, and returns to the initial value 14.7 s after burst onset.

Vasodilation Changes During Burst and Suppression

Calculation of the VDI for the increasing ICP segments had a median of 0.56 (TBI 0.56 mmHg, SAH 0.54 mmHg), and an interquartile range of 0.31 (TBI 0.30, SAH 0.28). This VDI was significantly higher than random for the two patients combined, but not for the TBI or SAH patient individually ($p < 0.001$). The magnitude of the VDI correlated with burst duration (All $\rho = 0.26$ $p < 0.001$, TBI $\rho = 0.28$ $p < 0.001$, SAH $\rho = 0.58$ $p < 0.01$).

Calculation of the VDI for time-aligned ICP segments on a sliding window allowed the characterization of the vasodilation response after an EEG burst (Fig. 5). The VDI was significantly higher than random from burst onset ($t = 0$ s) to $t = 3$ s. This was followed by a period from $t = 4$ s to $t = 7$ s, and $t = 9$ s where the VDI was significantly lower than random.

Discussion

In this study, we found that EEG and ICP, two signals used in the treatment of critical brain injury patients, could be related through the mechanism of neurovascular coupling. Our data show that the brief periods of electrical activity detected by EEG in burst-suppressed patients are followed by transient increases in ICP, and that the ICP increase and subsequent decrease are directly correlated with the durations of the burst and the suppression intervals, respectively. Moreover, we demonstrated that the VDI, an indicator of vasodilation, is also correlated to the duration of the burst and has a period of elevation that coincides with the timing of the EEG burst.

The role of neurovascular coupling is important, as the brain has little energy reserve and requires a constant supply of blood containing O_2 and glucose to sustain neural function. As neural activity of the brain varies, a tight regulation of CBF through neurovascular mechanisms is necessary to accommodate the metabolic demands of its cellular constituents. However, injury to the brain, such as trauma or hemorrhage, can result in a disruption of neurovascular coupling.

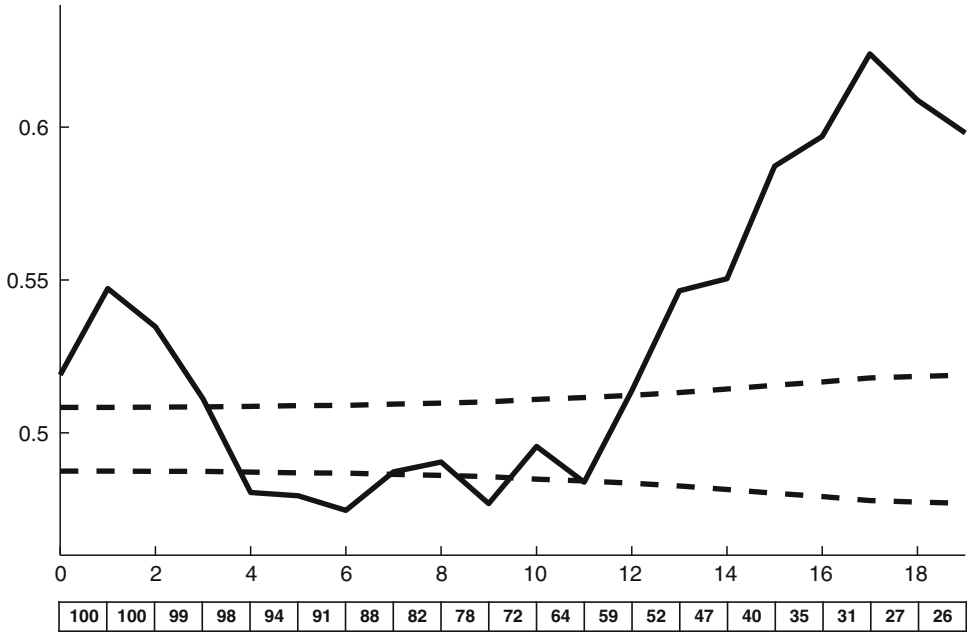

Fig. 5 The generalized VDI curve (*solid line*) compared to the mean value necessary to achieve statistical significance (*dashed line*). Table below shows the percentage of the original 309 ICP segments contributing to the mean VDI curve. Results were equivalent using non-parametric statistical tests (not shown)

Studies on pathological neurovascular coupling have identified CBF changes during epileptic activity and cortical spreading depression (CSD), typically characterized by profound hyperemia followed by persistent oligemia. This pattern has been demonstrated with CSDs in animal models [14, 15, 19] and reported in humans [18]. Similarly a preictal increase in CBF has been observed in patients with refractory epilepsy using single photon emission computed-tomography (SPECT) [4].

In the case of aSAH or ischemic stroke, the increased depolarization of CSD results in a significant decrease in CBF [13]. This has been demonstrated in animal models of subarachnoid hemorrhage using laser speckle flowmetry by Shin et al. [22], and in cerebral ischemia following middle cerebral artery occlusion by Strong et al. [25]. This is suggested by another study by Woitzik et al., which found evidence of delayed cerebral ischemia in aSAH patients with no angiographic evidence of vasospasm, but did experience CSDs [30]. This inverted neurovascular coupling after aSAH has also been observed using laser Doppler flowmetry (LDF) during ictal epileptic activity [29]. While these studies provide insight into pathological neurovascular coupling in the acute period following an injury, the reliance on additional and unconventional monitoring modalities has limited the studies on human patients.

The traditional techniques for measuring neurovascular coupling include functional magnetic resonance imaging (fMRI), positron emission tomography (PET), and SPECT. While these modalities provide a high degree of spatial and temporal resolution, they are cumbersome, require transporting patients out of the ICU, and can only be used intermittently.

Other, more continuous modalities such as LDF and NIRS have been used to some success in ICU. One study by Roche-Labarbe et al. [21] investigated the relationship between EEG and NIRS in premature neonates and found that the concentration of oxygenated hemoglobin increased and subsequently decreased following bursts of high electrical activity. Another study by Lescott et al. explored the relationship between EEG and ICP and found that the spectral edge frequency correlated with naturally occurring Lundberg oscillations in TBI patients [16].

Other groups have investigated neurovascular coupling in burst-suppressed animal models and humans. A study by Golanov et al. using mice burst-suppressed with isoflurane found consistent elevations in CBF measured by LDF following electrocortical bursts (Golanov, Yamamoto, & Reis, 1994). Another study on burst-suppressed mice by Liu et al. [17] demonstrated similar results using EEG to measure neural activity with LDF and fMRI BOLD signal to measure CBF changes. However, with the exception of the work by Roche-Labarbe et al. that took advantage of the naturally suppressed EEG rhythms in premature neonates, the study of neurovascular coupling during burst suppression has been primarily limited to animal models.

In this study, we utilized EEG and ICP signals to investigate neurovascular coupling in acute brain injury patients, while focusing on time points where they were heavily burst-suppressed allowing us to analyze the two signals in terms of a stimulus (burst) and response (post-burst ICP). Taking advantage of the multi-modality monitoring of the neurocritical care unit at UCLA, we identified two patients that received both depth EEG and ICP monitoring continuously and simultaneously while also being

burst suppressed with pentobarbital. While having a small cohort of patients, we were interested in providing an initial characterization of the ICP and EEG signals in order to develop a preliminary understanding of their relationship upon which to base future studies involving larger cohorts. While this preliminary study is limited by the sample size, we found statistically significant transient elevations in ICP following EEG burst that corresponds to the data obtained using NIRS [21], LDF [8], and fMRI [17].

By comparing the ICP immediately following an EEG burst, and how it behaves during the suppression interval, we were able to analyze these results within the context of neurovascular coupling and determine if these two signals are in fact coupled.

The initial categorization of the ICP response pattern after a burst found that the majority (80 %) of bursts were followed by an increase in ICP. After roughly half of the increasing ICP segments (63 %), the ICP peaked and began to decrease. That not every ICP increase eventually peaked shows that while the ICP may typically increase after a burst it does not always go down—suggesting that the increase in blood flow induced by the electrical activity did not completely satisfy the metabolic demand before the onset of the next burst. It was also found that of 309 bursts there was no instance of a spontaneous change from decreasing to increasing ICP, supporting our hypothesis that EEG burst activity induces an increase in ICP.

We found that the increase in ICP after a burst is significantly correlated with the duration of the burst. This correlation suggests that the ICP and EEG are proportionally coupled, where longer bursts create a greater metabolic demand and subsequent increase in blood flow. Using ICP segments time-aligned at burst onset and calibrated by shifting the mean to 0 mmHg, we characterized a general ICP response pattern (Fig. 4c). The generalized waveform demonstrated a parabolic pattern where the ICP increases before reaching a peak approximately 8 s after the EEG burst, and eventually returning to the initial value 14–15 s after the EEG burst. This generalized pattern has some clinical implications, as the protocol for administering barbiturates as a treatment for refractory intracranial hypertension has a target of 3–6 burst per minute [24, 28], and our results indicate the that burst frequency necessary to allow ICP to reach a steady state is four bursts per minute.

The second part of this study utilized our previously developed MOCAIP and PMTM algorithms [1, 11] for detecting vasodilation based on ICP pulse waveform changes. This technique allowed us to investigate whether the ICP changes after EEG busts were caused by the dilation and constriction of the distal vasculature. Looking at the immediate post-burst period, we found that the VDI values were significantly higher than those collected from random time points. This finding indicates that the ICP increases have pulse waveform patterns more consistent with those observed during hypercapnic vasodilation, suggesting that the ICP changes are caused by vascular dynamics. Moreover, the magnitude of the VDI was also slightly, but significantly correlated to the duration of the burst, providing further evidence that ICP and EEG signals reflect the proportional relationship between neural activity and blood flow in neurovascular coupling.

Characterizing the VDI changes after an EEG burst to produce a generalized VDI curve demonstrated that after the initial period of vasodilation, the ICP pulse waveform changes eventually become anti-vasodilatory. This finding supports our hypothesis that the decrease in ICP after a peak can be attributed to a reversal of the vasodilation. The later portion of the generalized VDI curve eventually increases to significant vasodilation. This increase could be an artifact, as from $t = 11$ s and on, only half of the bursts are represented, and will require additional data to investigate further.

Finally, it can be observed that the generalized VDI curve only stays above the randomness line from $t = 0$ s to $t = 3$ s, while the ICP curve peaks at $t = 8$ s. This discrepancy can be explained by the fact that PMTM measures the difference between ICP pulse waveforms, and is therefore best interpreted as the time derivative of vasodilation, where the peak just means that the speed of vasodilatation has reached maximum.

Limitations

As this study focused solely on patients with depth EEG monitoring, few cases were available. However, the techniques described here could be applied to surface EEG in future studies. Additionally, open extraventricular drains limited the number of time points where data collection was possible.

Conclusions

In this paper, we described a technique to integrate ICP and EEG, two signals monitored as part of the care of brain injury patients, based on the physiology of neurovascular coupling. A sophisticated integration of these two signals can allow us to study neurovascular coupling during the acute phase of brain injury management, and will help us understand and possibly detect and correct pathological neurovascular coupling

Acknowledgments XH support from the National Institutes of Health Award Number NS076738 and the University of California, San

Francisco Institute of Computational Health Sciences. NRG support from National Institute of neurological Disorders and Stroke of the National Institutes of Health under Award Number K23NS079477.

References

1. Asgari S, Bergsneider M, Hamilton R, Vespa P, Hu X. Consistent changes in intracranial pressure waveform morphology induced by acute hypercapnic cerebral vasodilatation. Neurocrit Care. 2011;15(1):55–62.
2. Asgari S, Gonzalez N, Subudhi AW, Hamilton R, Vespa P, Bergsneider M, Roach RC, Hu X. Continuous detection of cerebral vasodilatation and vasoconstriction using intracranial pulse morphological template matching. PLoS One. 2012;7(11): e50795. doi:10.1371/journal.pone.0050795.
3. Ayata C. Spreading Depression and Neurovascular Coupling. Stroke. 2013;44(6 suppl 1):S87–9. doi:10.1161/strokeaha.112.680264.
4. Baumgartner C, Serles W, Leutmezer F, Pataraia E, Aull S, Czech T, Pietrzyk U, Relic A, Podreka I. Preictal SPECT in temporal lobe epilepsy: regional cerebral blood flow is increased prior to electroencephalography-seizure onset. Journal of Nuclear Medicine: Official Publication, Society of Nuclear Medicine, 1998;39(6):978–82. Retrieved from http://www.ncbi.nlm.nih.gov/pubmed/9627329.
5. Bouma GJ, Muizelaar JP, Choi SC, Newlon PG, Young HF. Cerebral circulation and metabolism after severe traumatic brain injury: the elusive role of ischemia. J Neurosurg. 1991;75(5):685–93. doi:10.3171/jns.1991.75.5.0685.
6. Dreier JP. The role of spreading depression, spreading depolarization and spreading ischemia in neurological disease. Nat Med. 2011;17(4):439–47.
7. Füchtemeier M, Leithner C, Offenhauser N, Foddis M, Kohl-Bareis M, Dirnagl U, Lindauer U, Royl G. Elevating intracranial pressure reverses the decrease in deoxygenated hemoglobin and abolishes the post-stimulus overshoot upon somatosensory activation in rats. NeuroImage, 2010;52(2):445–454. Retrieved from http://www.sciencedirect.com/science/article/pii/S105381191000649X.
8. Golanov EV, YamamotoS, Reis DJ. Spontaneous waves of cerebral blood flow associated with a pattern of electrocortical activity. American Physiological Society Regulatory, Integrative and Comparative Physiology, 1994;266(1): R204–R214. Retrieved from http://ajpregu.physiology.org/content/266/1/R204.abstract.
9. Hart RG, Byer JA, Slaughter JR, Hewett JE, Easton DJ. Occurrence and Implications of Seizures in Subarachnoid Hemorrhage Due to Ruptured Intracranial Aneurysms. Neurosurgery, 1981;8(4): 417–421. Retrieved from http://journals.lww.com/neurosurgery/Fulltext/1981/04000/Occurrence_and_Implications_of_Seizures_in.2.aspx.
10. Hartings JA, Strong AJ, Fabricius M, Manning A, Bhatia R, Dreier JP, Mazzeo AT, Tortella FC, Bullock MR. Spreading depolarizations and late secondary insults after traumatic brain injury. J Neurotrauma. 2009;26(11):1857–66.
11. Hu X, Glenn T, Scalzo F, Bergsneider M, Sarkiss C, Martin N, Vespa P. Intracranial pressure pulse morphological features improved detection of decreased cerebral blood flow. Physiol Meas. 2010;31(5):679–95. doi:10.1088/0967-3334/31/5/006.
12. Hu X, Xu P, Scalzo F, Vespa P, Bergsneider M. Morpological clustering and analysis of continuous intracranial pressure. IEEE Trans Biomed Eng. 2009;56(3):696–705.
13. Koide M, Sukhotinsky I, Ayata C, Wellman GC. Subarachnoid hemorrhage, spreading depolarizations and impaired neurovascular coupling. Stroke Research and Treatment. 2013;2013: 819340. doi:10.1155/2013/819340.
14. Lauritzen M, Jørgensen MB, Diemer NH, Gjedde A, Hansen AJ. Persistent oligemia of rat cerebral cortex in the wake of spreading depression. Annals of Neurology. 1982;12(5):469–74. doi:10.1002/ana.410120510.
15. Leao AAP. Pial circulation and spreading depression of activity in the cerebral cortex. J Neurophysiol, 1944; 7(6):391–396. Retrieved from http://jn.physiology.org/content/7/6/391.citation.
16. Lescot T, Naccache L, Bonnet MP, Abdennour L, Coriat P, Puybasset L. The relationship of intracranial pressure Lundberg waves to electroencephalograph fluctuations in patients with severe head trauma. Acta Neurochirurgica. 2005;147(2):125–9. doi:10.1007/s00701-004-0355-8.
17. Liu X, Zhu X-H, Zhang Y, Chen W. Neural origin of spontaneous hemodynamic fluctuations in rats under burst suppression anesthesia condition. Cereb Cortex. 2011;21(2):374–84. doi:10.1093/cercor/bhq105.
18. Mayevsky A, Doron A, Manor T, Meilin S, Zarchin N, Ouaknine GE. Cortical spreading depression recorded from the human brain using a multiparametric monitoring system. Brain Research, 1996;740(1):268–274. Retrieved from http://www.sciencedirect.com/science/article/pii/S0006899396008748.
19. Mayevsky A, Weiss HR. Cerebral blood flow and oxygen consumption in cortical spreading depression. Journal of Cerebral Blood Flow and Metabolism. 1991;11(5):829–36. doi:10.1038/jcbfm.1991.142.
20. Miller JD, Becker DP, Ward JD, Sullivan HG, Adams WE, Rosner MJ. Significance of intracranial hypertension in severe head injury. J Neurosurg. 1977;47(4):503–16. doi:10.3171/jns.1977.47.4.0503.
21. Roche-Labarbe N, Wallois F, Ponchel E, Kongolo G, Grebe R. Coupled oxygenation oscillation measured by NIRS and intermittent cerebral activation on EEG in premature infants. NeuroImage, 2007; 36(3), 718–727. Retrieved from http://www.sciencedirect.com/science/article/pii/S1053811907003059.
22. Shin HK, Dunn AK, Jones PB, Boas DA, Moskowitz MA, Ayata C. Vasoconstrictive neurovascular coupling during focal ischemic depolarizations. Journal of Cerebral Blood Flow and Metabolism. 2006;26(8):1018–30. doi:10.1038/sj.jcbfm.9600252.
23. Steiner LA, Andrews PJD. Monitoring the injured brain: ICP and CBF. Br J Anaesth. 2006;97(1):26–38. doi:10.1093/bja/ael110.
24. Stover JF, Pleines UE, Morganti-Kossmann MC, Stocker R, Kossmann T. Thiopental attenuates energetic impairment but fails to normalize cerebrospinal fluid glutamate in brain-injured patients. Critical Care Medicine, 1999; 27(7), 1351–7. Retrieved from http://www.ncbi.nlm.nih.gov/pubmed/10446831.
25. Strong AJ, Anderson PJ, Watts HR, Virley DJ, Lloyd A, Irving EA, Nagafuji T, Ninomiya M, Nakamura H, Dunn AK, Graf R. Brain. 2007;130(4):995–1008. doi:10.1093/brain/awl392.
26. Vespa PM, Nuwer MR, Nenov V, Ronne-Engstrom E, Hovda DA, Bergsneider M, Kelly DF, Martin NA, Becker DP. Increased incidence and impact of nonconvulsive and convulsive seizures after traumatic brain injury as detected by continuous electroencephalographic monitoring. J Neurosurg. 1999;91(5):750–60. doi:10.3171/jns.1999.91.5.0750.
27. Westbrook LE, Devinsky O, Geocadin R. Nonepileptic seizures after head injury. Epilepsia. 1998;39(9):978–82. doi:10.1111/j.1528-1157.1998.tb01447.x.
28. Winer JW, Rosenwasser RH, Jimenez F. Electroencephalographic activity and serum and cerebrospinal fluid pentobarbital levels in determining the therapeutic end point during barbiturate coma. Neurosurgery, 1991; 29(5), 739–41; discussion 741–2. Retrieved from http://www.ncbi.nlm.nih.gov/pubmed/1961405.
29. Winkler MKL, Chassidim Y, Lublinsky S, Revankar GS, Major S, Kang E-J, Oliveira-Ferreira AI, Woitzik J, Sandow N, Scheel M, Friedman A, Dreier JP. Impaired neurovascular coupling to ictal epileptic activity and spreading depolarization in a patient

with subarachnoid hemorrhage: possible link to blood-brain barrier dysfunction. Epilepsia. 2012;53(6):22–30. doi:10.1111/j.1528-1167.2012.03699.x.

30. Woitzik J, Dreier JP, Hecht N, Fiss I, Sandow N, Major S, Winkler M, Dahlem YA, Manville J, Diepers M, Muench E, Kasuya H, Schmiedek P, Vajkoczy P. Delayed cerebral ischemia and spreading depolarization in absence of angiographic vasospasm after subarachnoid hemorrhage. J Cereb Blood Flow Metab. 2012;32(2):203–12. doi:10.1038/jcbfm.2011.169.